

## UTILIZATION OF BAGASSE ASH FOR THE PREPARATION OF SILICA AEROGEL/MgO COMPOSITES THROUGH AMBIENT-PRESSURE DRYING

*Istighfarin Meilidya Azhar<sup>1</sup>, Nazriati<sup>1\*</sup>, Irma Kartika Kusumaningrum<sup>1</sup>*

<sup>1</sup>Department of Chemistry, Faculty of Mathematics and Natural Sciences, Universitas Negeri Malang, Jl. Semarang No. 5, Malang City, 65145, Indonesia

\*Corresponding author: [nazriati.fmipa@um.ac.id](mailto:nazriati.fmipa@um.ac.id)

### Abstract

*This study presents the preparation of silica aerogel/MgO composites using bagasse ash as a silica source and  $\text{MgCl}_2 \cdot 6\text{H}_2\text{O}$  as the MgO precursor. Sodium silicate was extracted from bagasse ash and converted into silicic acid through ion-exchange treatment. Silica aerogel formation was achieved through gelation, followed by surface modification using TMCS and HMDS. Magnesium oxide was incorporated via co-precipitation with  $\text{MgCl}_2 \cdot 6\text{H}_2\text{O}$  and subsequently stabilized through calcination. The composites were characterized using FTIR, XRD, and BET-BJH analyses. XRD results revealed a hybrid amorphous-crystalline structure, with silica predominantly in the amorphous phase and MgO in the crystalline phase. BET analysis showed a pore volume of  $0.50 \text{ cm}^3/\text{g}$  and a specific surface area of  $121.99 \text{ m}^2/\text{g}$ , while the pore-size distribution confirmed its mesoporous nature. FTIR spectra indicated the presence of functional groups corresponding to Si-O-Si, Si-C, C-H, and Mg-O, confirming the successful integration of MgO into the silica aerogel framework. These findings demonstrate the successful preparation of silica aerogel/MgO composites from bagasse ash under ambient-pressure drying conditions.*

**Keywords:** silica aerogel; MgO; composite; bagasse ash

### Introduction

The utilization of agro-industrial residues as precursors for advanced functional materials has gained significant attention because of their environmental and economic benefits. Among these residues, bagasse ash, the by-product of the sugarcane milling process, is particularly rich in silica and therefore offers a renewable alternative to commercial silica sources. Converting this waste into value-added materials also reduces disposal challenges commonly associated with agro-industrial residues.

A key step in preparing stable silica aerogels under ambient pressure is the

silylation of surface silanol groups (Si-OH) into siloxane linkages (Si-O-Si). This modification enhances hydrophobicity and minimizes structural collapse caused by capillary forces during drying (Di Luigi et al., 2022; Zemke et al., 2023; Niculescu et al., 2024). As a result, the dried aerogels retain a three-dimensional mesoporous framework with distinctive features such as large pore volume, low thermal conductivity, and high surface area (Nazriati et al., 2014).

Silica aerogels can be synthesized through a sol-gel route using sodium silicate extracted from bagasse ash, followed by surface silylation to preserve mesostructural integrity during ambient

drying (Rahayu et al., 2020). Reagents such as trimethylchlorosilane (TMCS) and hexamethyldisilazane (HMDS) replace surface  $-OH$  groups with hydrophobic  $-CH_3$  groups, resulting in improved structural stability and functional performance. Previous reports have shown that bagasse-derived silica aerogels may exhibit surface areas of 540–1114  $m^2/g$  and pore volumes up to 2.16  $cm^3/g$  (Nazriati et al., 2014).

Nevertheless, pristine silica aerogels, despite their exceptionally high surface area and porosity (Huynh et al., 2021), exhibit limited affinity toward certain complex dye molecules, particularly under hydrophobic conditions or when the surface is insufficiently functionalized (Goryunova et al., 2023). To address this limitation, recent studies have explored the incorporation of metal oxides. Magnesium oxide (MgO) is especially promising because its surface  $O^{2-}$  sites provide electrostatic interactions with cationic dye moieties (e.g.,  $N^+$  groups in malachite green), while  $Mg^{2+}$  centers can bond with silica silanol groups, resulting in a synergistic adsorption mechanism (Wang et al., 2023; Gui et al., 2015).

In the present work, silica aerogel/MgO composites were synthesized using bagasse ash as the silica precursor and  $MgCl_2 \cdot 6H_2O$  as the MgO source. The novelty of this study lies in three main aspects: (i) the utilization of bagasse ash as a low-cost silica precursor; (ii) the application of ambient-pressure drying combined with surface modification to maintain mesoporosity; and (iii) the successful incorporation of MgO into the silica aerogel framework. The resulting composites were examined by FTIR (Fourier transform infrared), XRD (X-ray diffraction), and BET-BJH analyses to elucidate their structural and surface properties. This study presents the first demonstration of bagasse-ash-derived silica aerogels integrated with MgO under ambient-pressure drying conditions.

## Experimental Section

### Materials

The bagasse ash used in this study was obtained from PG Kebon Agung, a sugar mill located in Malang, Indonesia. The chemicals used were sodium hydroxide (NaOH, p.a., Merck), ammonium hydroxide ( $NH_4OH$ , 25%, Merck), magnesium chloride hexahydrate ( $MgCl_2 \cdot 6H_2O$ , p.a., Merck), hexamethyldisilazane (HMDS, p.a., Merck), trimethylchlorosilane (TMCS, p.a., Merck), cation-exchange resin (Amberlite HPR 1100 Na), pH indicator paper (Merck), and demineralized water.

### Instruments

XRD patterns were recorded using a PANalytical X'Pert PRO instrument operated with Cu K $\alpha$  radiation ( $\lambda = 1.5406 \text{ \AA}$ ) over a  $2\theta$  scan range of 10–90°. The specific surface area and pore characteristics were analyzed using a Micromeritics Tristar II Plus 3.04 surface area and pore volume analyzer. The samples were degassed at 573 K for 3 hours, while  $N_2$  adsorption-desorption isotherms were measured at 77 K. FTIR spectra were obtained using a Bruker Alpha spectrometer within the 500–4000  $cm^{-1}$  range using KBr pellets.

### Procedure

#### Preparation of Bagasse Ash

The bagasse ash was oven-dried at 105°C for 4 hours to obtain a completely dry material. After cooling to ambient temperature, the ash was sieved to achieve a uniform particle size. The resulting dry, uniformly sized ash was used as the precursor for sodium silicate preparation.

#### Silica Extraction and Sodium Silicate Production

In a 250 mL Erlenmeyer flask, 10 g of dry bagasse ash were suspended in 60 mL of 2 N NaOH solution. The mixture was heated to boiling and maintained under magnetic stirring for 1 hour. After cooling to room temperature, the mixture was filtered using Whatman 41 filter paper. The filtrate, corresponding to sodium silicate, was collected for further processing (Nazriati et al., 2014).

### Preparation of Silicic Acid

A mixture was prepared by combining 10 mL of sodium silicate solution with 30 mL of ion-exchange resin (1:3) in a 100 mL beaker. The solution was stirred magnetically for 30 minutes until the pH stabilized at 2. It was then filtered, and the resulting filtrate (silicic acid) was collected (Nazriati et al., 2014).

### Synthesis of Silica Aerogel

In a beaker, 10 mL of silicic acid was mixed with 0.3 mL of TMCS and stirred for several minutes. Next, 0.6 mL of HMDS was added, followed by continued stirring. To strengthen the network structure, the obtained gel was aged for 18 hours at room temperature and atmospheric pressure. After gelation, the gel was washed with demineralized water until a neutral pH was reached. The silica aerogel was produced by drying the gel in an oven at 80°C for 24 hours (Nazriati et al., 2014).

### Synthesis of Silica Aerogel/MgO Composite

The silica aerogel/MgO composite was synthesized via a co-precipitation method. A solution was prepared by mixing 10 mL of 3 M  $\text{NH}_4\text{OH}$ , 3 g of  $\text{MgCl}_2 \cdot 6\text{H}_2\text{O}$ , and 300 mL of distilled water, followed by magnetic stirring at 300 rpm for 30 minutes. Subsequently, 1 g of silica aerogel from the previous step was added. The suspension was stirred continuously on a hotplate at 25°C and 500 rpm for 24 hours, yielding a precipitate and a filtrate. The solid fraction was separated and washed repeatedly with demineralized water until a neutral pH was achieved, then dried at 80°C for 2 hours. It was subsequently calcined in a muffle furnace at 300°C for 1 hour and at 525°C for 2.5 hours to convert  $\text{Mg}(\text{OH})_2$  adhering to the aerogel surface into  $\text{MgO}$ .

### Characterization of Silica Aerogel/MgO Composite

The synthesized composite was characterized using XRD, BET-BJH surface area and pore analysis, and FTIR spectroscopy.

## Results and Discussion

### Preparation of Bagasse Ash

The bagasse ash appeared black-gray and had the texture of a coarse powder. Analysis showed that the ash obtained from PT PG Kebon Agung, Malang, contained 61.5% w/w  $\text{SiO}_2$ . The ash was oven-dried at 105°C for 4 hours to remove residual moisture and then sieved to obtain a uniform particle size, as illustrated in Figure 1.



**Figure 1.** Bagasse ash with uniform particle size

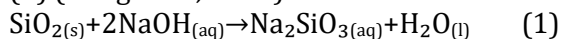
### Silica Extraction and Sodium Silicate Production

Sodium silicate was produced by treating the ash with  $\text{NaOH}$  solution, which promoted the solubilization of silicate species. The silica in the bagasse ash was thereby converted into soluble sodium silicate (Nazriati et al., 2014). After heating, the solution was cooled to room temperature and filtered using a Büchner funnel. The resulting filtrate was a brownish-gold sodium silicate solution with a pH of approximately 12 (see Figure 2).



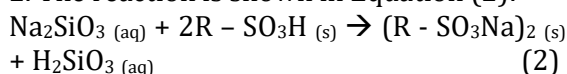
**Figure 2.** Sodium silicate filtrate

The extraction involved the conversion of  $\text{SiO}_2$  into silicate ions, as shown in Equation (1) (Kong et al., 2024):

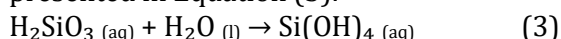


### Production of Silicic Acid

A mixture of 10 mL of sodium silicate solution and 30 mL of ion-exchange resin (1:3 ratio) was used to produce silicic acid, followed by magnetic stirring for 30 minutes. The ion-exchange process involved replacing  $\text{Na}^+$  with  $\text{H}^+$  ions supplied by the resin. Because of its larger ionic radius,  $\text{Na}^+$  was more strongly retained by the resin, which subsequently released  $\text{H}^+$  ions. This mechanism facilitated the conversion of sodium silicate into silicic acid (Akkaya et al., 2024). The mixture was then filtered, producing a pale-yellow filtrate with a pH of 2. The reaction is shown in Equation (2):



Condensation polymerization commonly occurs in silicic acid solutions, where  $\text{Si}-\text{OH}$  groups react to generate  $\text{Si}-\text{O}-\text{Si}$  bonds with the elimination of water. The reaction is presented in Equation (3):



### Silica Aerogel Synthesis

The silicic acid solution was modified with 0.3 mL of TMCS and stirred for 30 minutes at room temperature to remove residual water that might cause shrinkage. The reaction between silanol groups and TMCS is shown in Figure 3 (Halim et al., 2024). HMDS (0.6 mL) was then added and stirred briefly (5 minutes) until gelation occurred. The TMCS:HMDS ratio of 0.3:0.6 mL was selected because previous studies reported that this ratio yielded the highest specific surface area ( $1114 \text{ m}^2/\text{g}$ ) among tested conditions (Nazriati et al., 2014). HMDS contributed to gel formation by increasing hydrophobicity, thereby improving resistance to water and solvents. The HMDS reaction scheme is shown in Figure 4 (Veselova et al., 2024).

The combined use of TMCS and HMDS aimed to prevent shrinkage during ambient drying by replacing surface silanol ( $\text{Si}-\text{OH}$ ) groups with hydrophobic  $-\text{CH}_3$  groups (Rahayu et al., 2020). These non-polar groups enhanced the water resistance of the resulting silica aerogel.

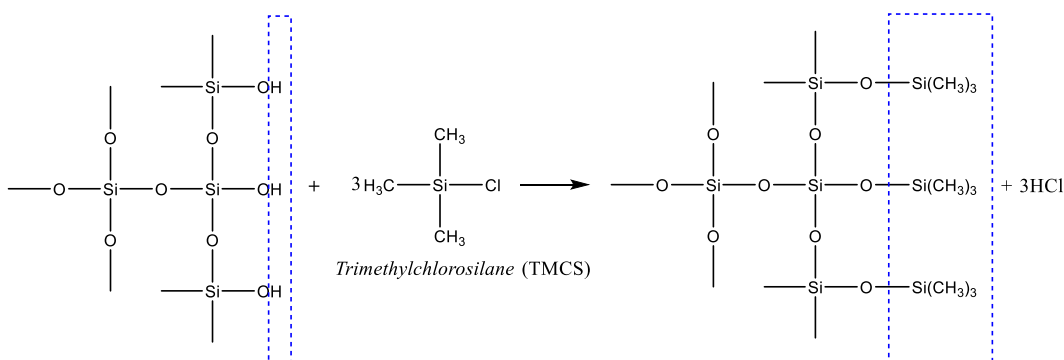


**Figure 3.** Reaction scheme of silica surface modification using TMCS

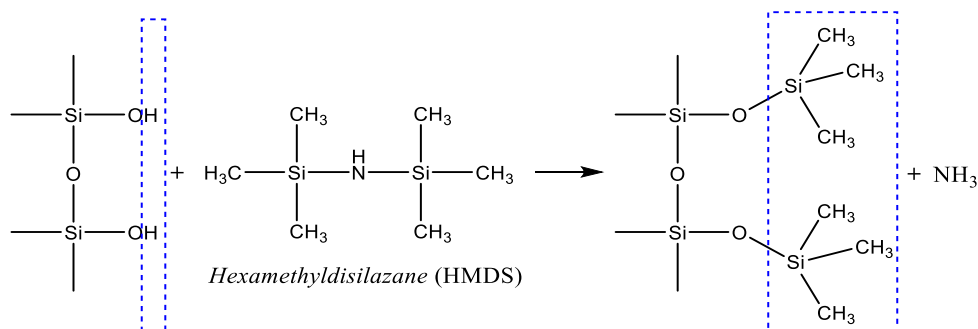


**Figure 4.** Reaction scheme of silica surface modification using HMDS

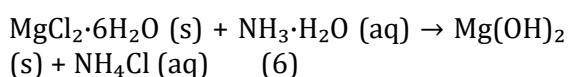
The formed gel was aged for 18 hours at ambient temperature and atmospheric pressure to strengthen the network structure. It was then rinsed several times with demineralized water until reaching a neutral pH. The material was oven-dried at 80°C for 24 hours under ambient conditions. The final product was a white silica aerogel solid (see Figure 5).



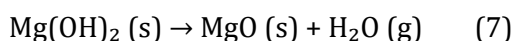
**Figure 5.** White dried silica aerogel

### Synthesis of Silica Aerogel/MgO Composite

The silica aerogel/MgO composite was synthesized by mixing  $\text{NH}_4\text{OH}$ ,  $\text{MgCl}_2 \cdot 6\text{H}_2\text{O}$ , and distilled water. At ambient temperature, the mixture was subjected to magnetic stirring at 300 rpm for 1 hour to promote the formation of  $\text{Mg}(\text{OH})_2$ , as shown in Equation (6):



Next, 1 g of silica aerogel obtained from the previous step was added and stirred at 500 rpm for 24 hours at room temperature to allow  $\text{Mg}(\text{OH})_2$  to attach to the aerogel surface. The suspension was aged for 24 hours, after which the resulting precipitate was washed several times with demineralized water until neutral and then dried at 80°C for 2 hours. The dried powder was calcined at 300°C for 1 hour, followed by heating at 525°C for 2.5 hours to ensure complete conversion of  $\text{Mg}(\text{OH})_2$  to MgO while maintaining the silica structure. The thermal conversion is shown in Equation (7) (Pei et al., 2015):



The final composite appeared as a white solid (see Figure 6).



**Figure 6.** Silica Aerogel/MgO Composite

The total yield of the composite after calcination was 1.1 g, consisting of approximately 1.0 g silica aerogel (90.9% w/w) and 0.1 g MgO (9.1% w/w). Based on molar calculations, this corresponded to 0.0166 mol Si (as  $\text{SiO}_2$ ) and 0.00248 mol MgO, giving a Si/Mg molar ratio of 6.7:1.

### Characterization of Silica Aerogel/MgO Composite

#### XRD (X-Ray Diffraction)

XRD analysis was performed to confirm the successful incorporation of MgO into the silica aerogel matrix and to identify the crystallinity and phase structure of the composite. The broad amorphous hump at approximately  $2\theta = 22^\circ$  indicated the presence of the silica aerogel framework, while sharp diffraction peaks above  $30^\circ$ , particularly at  $36.9^\circ$ ,  $42.9^\circ$ , and  $62.3^\circ$ , confirmed that MgO remained in a crystalline state and was effectively dispersed within the silica matrix. The coexistence of the amorphous silica signal and the crystalline MgO reflections demonstrated the formation of a hybrid amorphous-crystalline structure. Specifically, the amorphous peak of silica was observed at  $21.8^\circ$  (Jo et al., 2021). Consistent with previous studies, characteristic diffraction features of  $\text{SiO}_2$  and  $\text{SiO}_2$ -MgO composites appeared in the regions of  $40$ – $45^\circ$  and  $60$ – $65^\circ$  (Wang et al., 2023). Figure 7 presents the XRD pattern of the material.

#### BET (Brunauer-Emmett-Teller) and BJH (Barrett-Joyner-Halenda)

The specific surface area and pore characteristics were evaluated using BET and BJH analyses. Figure 8 shows the nitrogen adsorption-desorption isotherms



measured at 77 K for silica aerogel and the silica aerogel/MgO composite. The surface area and pore volume of pure silica aerogel were recorded at 635.61 m<sup>2</sup>/g and 0.974 cm<sup>3</sup>/g, respectively, which are considerably higher than those of the composite (121.99 m<sup>2</sup>/g and 0.504 cm<sup>3</sup>/g). This reduction is attributed to the partial blockage of silica pores by MgO particles, which decreases available adsorption sites and overall pore volume. In contrast, the average pore radius increased significantly from 27.99 Å in the aerogel to 65.17 Å in the composite, suggesting the formation of larger interparticle voids that replace the smaller, densely packed pores. This structural adjustment results in reduced surface area alongside an increase in average pore size.

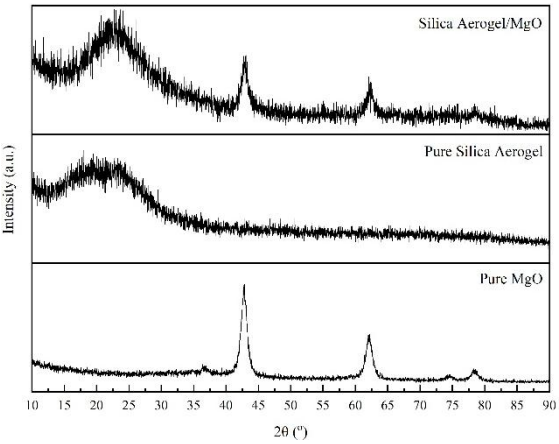


**Figure 7.** XRD pattern of pure silica aerogel, pure MgO, and silica aerogel/MgO composite

**Table 1.** Physical Properties of Silica Aerogel and Silica Aerogel/MgO

Parameters	Silica Aerogel	Silica Aerogel/MgO
BET Surface Area (m <sup>2</sup> /g)	635.61	121.99
Pore Volume (cm <sup>3</sup> /g)	0.97	0.50
BJH Pore Radius (Å)	27.99	65.17

According to IUPAC classification, both silica aerogel and silica aerogel/MgO are mesoporous materials. Their isotherms correspond to type IV curves with H3-type hysteresis loops, which are typical of open channel-like mesopores commonly

observed in silica-based composites. Similar type IV isotherms with H3 hysteresis have been reported for SiO<sub>2</sub>@MgO composites synthesized from microsilica precursors (Pei et al., 2015).

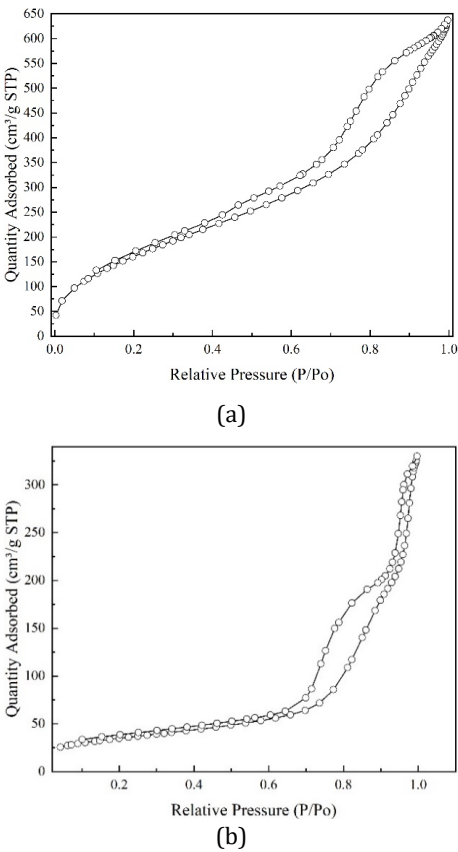


**Figure 8.** Adsorption-desorption curve: (a) silica aerogel, (b) silica aerogel/MgO.

**FTIR (Fourier Transform Infrared)**

As shown in Figure 9, the FTIR analysis produced spectra for pure silica aerogel and the silica aerogel/MgO composite. Both samples exhibited a broad absorption band at 3437 cm<sup>-1</sup>, assigned to the stretching vibration of surface silanol groups (Si-OH), and a band at 1635 cm<sup>-1</sup> corresponding to the bending mode of adsorbed water molecules, consistent with Wang et al. (2023). A band at 2960 cm<sup>-1</sup> indicates C-H stretching, while the absorption at 1439 cm<sup>-1</sup> is attributed to C-H bending vibrations. An absorption peak at 1068 cm<sup>-1</sup> represents asymmetric Si-O-Si stretching, with an additional band at 802 cm<sup>-1</sup> corresponding to Si-C vibrations, in agreement with Nazriati et al. (2014). Notably, the composite spectrum shows an

additional peak at  $499\text{ cm}^{-1}$ , assigned to Mg–O stretching. This finding aligns with Al Musayeib et al. (2024), who reported a similar Mg–O band at  $495\text{ cm}^{-1}$ . The presence of this band confirms the successful incorporation of MgO into the silica aerogel framework and the formation of the composite structure.

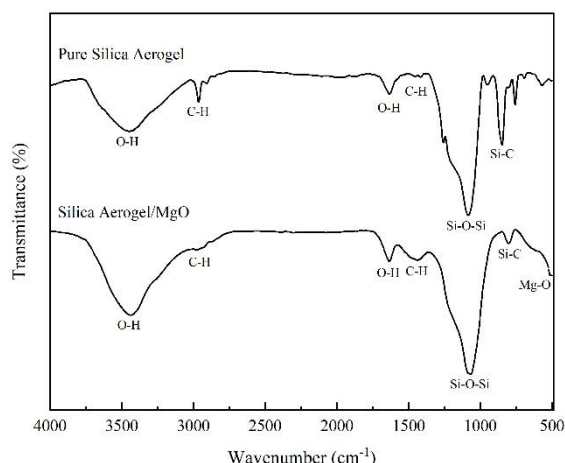


**Figure 9.** FTIR spectra of pure silica aerogel and silica aerogel/MgO

## Conclusion

The silica aerogel/MgO composite was successfully synthesized from bagasse ash under ambient-pressure conditions with surface modification using TMCS and HMDS. The synthesis pathway involved silica extraction, ion exchange to obtain silicic acid, gelation, and the incorporation of MgO through precipitation and calcination. Characterization confirmed a hybrid amorphous–crystalline structure, with silica contributing to the amorphous phase and MgO retaining its crystalline form. BET and BJH analyses showed a specific surface area of  $121.99\text{ m}^2/\text{g}$  and mesoporous pore diameters, while FTIR identified functional groups characteristic of silica (C–H, Si–C, Si–O–Si) and MgO (Mg–O). These findings demonstrate that silica aerogel/MgO composites with well-defined structural and surface features can be effectively synthesized from bagasse ash under ambient-pressure conditions.

## Acknowledgments

The authors gratefully acknowledge the support provided by Universitas Negeri Malang through non-APBN grant funding.

## References

- Akkaya, B., Aslan, J., Taşdemir, R., Erdem, İ., & Gönen, M. (2024). Colloidal Silica Production with Resin from Sodium Silicate and Optimization of Process. *Open Journal of Nano*, 9(1), 1-10.  
<https://doi.org/10.56171/ojn.1402531>
- Al Musayeib, N. M., Amina, M., Maqsood, F., Bokhary, K. A., & Alrashidi, N. S. (2024). Biogenic synthesis of photosensitive magnesium oxide nanoparticles using citron waste peel extract and evaluation of their antibacterial and anticarcinogenic potential. *Bioinorganic Chemistry and Applications*, 2024(1), 8180102.  
<https://doi.org/10.1155/2024/8180102>
- Di Luigi, M., Guo, Z., An, L., Armstrong, J. N., Zhou, C., & Ren, S. (2022). Manufacturing silica aerogel and cryogel through ambient pressure and freeze drying. *RSC advances*, 12(33), 21213-21222.
- Goryunova, K., Gahramanli, Y., & Gurbanova, R. (2023). Adsorption properties of silica aerogel-based materials. *RSC advances*, 13(27), 18207-18216.  
<https://doi.org/10.1039/d3ra02462>
- Gui, C. X., Li, Q. J., Lv, L. L., Qu, J., Wang, Q. Q., Hao, S. M., & Yu, Z. Z. (2015). Core-shell structured MgO@ mesoporous silica spheres for enhanced adsorption of methylene blue and lead ions. *RSC Advances*, 5(26), 20440-20445.  
<https://doi.org/10.1039/c5ra02596f>
- Halim, Z. A. A., Awang, N., Ahmad, N., & Yajid, M. A. M. (2024). Effects of silane concentration on hydrophobic conversion of rice husk-derived silica aerogels prepared by supercritical drying. *Biomass Conversion and Biorefinery*, 14(14), 15811-15821.  
<https://doi.org/10.1007/s13399-022-03710-8>

- <https://doi.org/10.1039/D2RA03325A>  
Huynh, J., Palacio, R., Allavena, A., Gallard, H., Descostes, M., Mamède, A. S., ... & Batonneau-Gener, I. (2021). Selective adsorption of U (VI) from real mine water using an NH<sub>2</sub>-functionalized silica packed column. *Chemical Engineering Journal*, 405, 126912. <https://doi.org/10.1016/j.cej.2020.126912>
- Jo, S. E., Choi, J. W., & Choi, S. J. (2021). Synthesis of silver-impregnated magnetite mesoporous silica composites for removing iodide in aqueous solution. *Toxics*, 9(8), 175. <https://doi.org/10.3390/toxics9080175>
- Kong, D., Gao, Y., Song, S., & Jiang, R. (2024). Kinetics and Mechanism of SiO<sub>2</sub> Extraction from Acid-Leached Coal Gangue Residue by Alkaline Hydrothermal Treatment. *Materials*, 17(17), 4168. <https://doi.org/10.3390/ma17174168>
- Nazriati, N., Setyawan, H., Affandi, S., Yuwana, M., & Winardi, S. (2014). Using bagasse ash as a silica source when preparing silica aerogels via ambient pressure drying. *Journal of non-crystalline solids*, 400, 6-11. <https://doi.org/10.1016/j.jnoncrysol.2014.04.027>
- Niculescu, A. G., Tudorache, D. I., Bocioagă, M., Mihaiescu, D. E., Hadibarata, T., & Grumezescu, A. M. (2024). An updated overview of silica aerogel-based nanomaterials. *Nanomaterials*, 14(5), 469. <https://doi.org/10.3390/nano14050469>
- Pei, Y., Wang, M., Tian, D., Xu, X., & Yuan, L. (2015). Synthesis of core-shell SiO<sub>2</sub>@MgO with flower like morphology for removal of crystal violet in water. *Journal of colloid and interface science*, 453, 194-201. <https://doi.org/10.1016/j.jcis.2015.05.003>
- Rahayu, W., Muthomimah, S., Sumari, S., & Nazriati, N. (2020). Effect of sonication time on characteristics of synthesized silica aerogel activated carbon nanocomposite based on bagasse ash. In *IOP Conference Series: Materials Science and Engineering* (Vol. 833, No. 1, p. 012088). IOP Publishing. <https://doi.org/10.1088/1757-899X/833/1/012088>
- Veselova, V. O., Kottsov, S. Y., Golodukhina, S. V., Khvoshchevskaya, D. A., & Gajtko, O. M. (2024). Hydrophilic and Hydrophobic: Modified GeO<sub>2</sub> Aerogels by Ambient Pressure Drying. *Nanomaterials*, 14(18), 1511. <https://doi.org/10.3390/nano14181511>
- Wang, M., Jiao, Y., Li, N., & Su, Y. (2023). Synthesis of a SiO<sub>2</sub>-MgO composite material derived from yellow phosphorus slag with excellent malachite green adsorption activity. *Journal of Alloys and Compounds*, 969, 172344. <https://doi.org/10.1016/j.jallcom.2023.172344>
- Zemke, F., Gonthier, J., Scoppola, E., Simon, U., Bekheet, M. F., Wagermaier, W., & Gurlo, A. (2023). Origin of the springback effect in ambient-pressure-dried silica aerogels: the effect of surface silylation. *Gels*, 9(2), 160. <https://doi.org/10.3390/gels9020160>